Available online at www.sciencedirect.com

jmr&t Journal of Materials Research and Technology

www.jmrt.com.br

Original Article

Effect of biodiesel components on its lubrication performance

Fashe Li[a,b], Zuowen Liu[a,b,*], Zihao Ni[a,b], Hua Wang[a,b]

[a] Faculty of Metallurgical and Energy Engineering, Kunming University of Science and Technology, Kunming 650106, China
[b] State Key Laboratory of Complex Nonferrous Metal Resources Clean Utilization, Kun-ming 650093, China

ARTICLE INFO

Article history:
Received 14 November 2018
Accepted 6 June 2019
Available online 12 July 2019

Keywords:
Biodiesel
Friction coefficient
Chemical composition
Abrasive spot diameter
Regression analysis
Oil feedstock

ABSTRACT

The composition of biodiesel significantly influences its lubrication performance. Gas chromatography, high frequency reciprocating friction, and wear test machines were used to determine the composition and abrasive spot diameter of biodiesels produced from fourteen different oil feedstocks. At the same time, the relationship between the grinding point diameter and chemical composition of biodiesel was quantified. The main components of the biodiesel are methyl stearate, methyl palmitate, methyl oleate, and methyl linoleate, with an average content of 92.18%. Among the various types of biodiesel, rubber seed methyl ester has a minimum grinding point diameter of 169.71 μm. Prickly ash methyl ester has the largest grinding point diameter of 187.35 μm. A linear correlation prediction model of wear point diameter was established (R = 0.91).

1. Introduction

The widespread use of fossil fuels in power plants, transport vehicles, generators, and mining equipment has resulted in higher energy consumption [1,2]. The devastating impacts of increasing consumption of fossil-oriented energy carriers have already gone well beyond the environmental sustainability. Climate change has, in fact, substantially endangered public health and these impacts are going to be far more comprehensive in the next decades [3–5].

The environmental pollution generated by fossil fuels is currently increasing [6]. Owing to the finite stock of fossil fuels and its negative impact on the environment, many countries across the world are now leaning toward renewable sources of energy such as solar energy, wind energy, biofuel, hydropower, geothermal, and ocean energy to ensure energy for the countries' development security [7]. Biodiesel is a biodegradable, renewable, clean, and environmentally friendly liquid fuel. It is lipid-derived fuel produced by transesterification in the presence of a suitable catalyst [8]. Biodiesel has established itself as a partial substitute for diesel in existing diesel engines despite some differences in the properties of two fuels [9]. Compared to conventional diesel, good lubricity is an important feature of biodiesel. It reduces friction and wear for sliding parts and prolongs the life of the engine. Fazal et al. [10] observed the

* *Corresponding author*. Liu e-mail:liuzuowen3@163.com
E-mails: asanli@foxmail.com (F. Li), liuzuowen3@163.com (Z. Liu).
https://doi.org/10.1016/j.jmrt.2019.06.011

wear and friction characteristics of palm oil biodiesel (B10, B20, B50, and B100) under constant load at different rotational speeds (600, 900, 1200, and 1500 rpm). The results showed that when the ratio of biodiesel increased, wear and friction decreased, and the addition of biodiesel led to the effective reduction of the wear and friction of the sliding parts. Kumar et al. [11] observed the wear and friction characteristics of jatropha biodiesel blends (20, 40, and 100% JOME) in a four-ball tester. The results revealed that the fuel showed better lubricity with the increase in the biodiesel concentration, and the decrease in the load and temperature. Lubricating properties of biodiesel are usually evaluated using high frequency reciprocating friction and wear testing machine (HFRR) [12–14]. Sulek et al. [15] used HFRR to study the tribological properties of rapeseed biodiesel. They observed that the coefficient of friction of B5 (diesel mixed with 5% rapeseed biodiesel) and B100 was lower than that of diesel, respectively.

Xiao et al. reported that wear scar sizes of steel balls for steel–steel contact decreased with increasing concentration of biodiesel [16]. Sukjit et al. [17] observed that reduction of unsaturated molecules in unsaturated fatty acid methyl ester (H-FAME) decreased sensitivity to humidity. Chourasia et al. [18] indicated that the wear of B20A4 fueled engine was substantially lower than that of the diesel fueled engine. A regression model was also proposed to predict wear of the engine. The proposed regression model can be taken one step further to predict the overall wear of the engine. The total concentration of various metals debris collected in the lube oil sample (predicted using regression model) was found to be 640 mg kg^{-1} and 420 mg kg^{-1} for diesel and B20A4, respectively.

Biodiesel components have an important impact on their performance, including cetane number (CN), oxidative stability, heat of vaporization (HV), etc. [19]. Hosseinpour et al. [20] estimated the CN of biodiesel from its FAMES profile. Geller et al. and Hu et al. [21] showed that the FAME composition of biodiesel plays an important role in lubricity. A more intense research on biodiesel composition and its corrected abrasive spot diameter can help objectively evaluate the quality of biodiesel, extend its activity and commercial application, and provide intellectual support for the national energy-saving and emission reduction strategy involving renewable energy. In this study, gas chromatography, high frequency reciprocating friction, and wear testing were used to measure the FAME composition and calibrate the abrasive spot diameter of 14 types of biodiesel. The influence of FAME content of biodiesel on its corrected abrasive spot diameter was analyzed by multiple linear regression analysis. The relationship between the diameter of the corrected grinding spot and the chemical composition of the biodiesel was quantified, which provides some guidance and practical significance for the research on the lubricating properties of biodiesel.

2. Materials and methods

2.1. Materials and reagents

Fourteen biodiesel samples (self-prepared), namely sunflower seed methyl ester (SSME), jatropha methyl ester (JME), camellia oleosa seed methyl ester (COSME), oryza sativa methyl ester (OSME), maize methyl ester (MME), canola methyl ester (CME), rapeseed methyl ester (RME), sesame methyl ester (SME), peanut methyl ester (PME), soya bean methyl ester (SBME), rubber seed methyl ester (RSME), prickly ash methyl ester (PAME), cooking oil biodiesel (OOB), and olive methyl ester (OME) were used in this study. The materials and reagents required for the test are listed in Table 1.

Table 1 – Materials and reagents.

Materials and reagents	Manufacturer
Nitrogen (99.99%)	Messer Gas Company Limited
Ultra-pure water	Ultrapure water generator (UK ELGA LabWater)
Acetone	Wuhan Yuancheng Technology Development Co., Ltd.
Petroleum ether	Borida Trade Co., Ltd.
95% ethanol	Tianjin Komiou Co., Ltd.
Methanol (HPLC grade)	Wuhan Yuancheng Technology Development Co., Ltd.
Linolenic methyl ester (HPLC grade)	Aladdin Reagent.
Oleic methyl ester (HPLC grade)	Aladdin Reagent
Palmitic methyl ester (HPLC grade)	Aladdin Reagent
Stearic methyl ester (HPLC grade)	Bailingwei Technology Co., Ltd.
Arachidic methyl ester (HPLC grade)	Bailingwei Technology Co., Ltd.
Behenic methyl ester (HPLC grade)	Bailingwei Technology Co., Ltd.
Wood tar acid methyl ester (HPLC grade).	Bailingwei Technology Co., Ltd.

2.2. Biodiesel preparation

Biodiesel samples were produced through transesterification with methanol in the presence of potassium hydroxide (KOH) as a base catalyst at 75 °C for 3 h. Upon the completion of the reaction, glycerol was decanted and the crude biodiesel phase was washed five times with distilled water at 60 °C. Subsequently, the purified biodiesel was dried in an oven at 100 °C for 2 h. The basic physicochemical properties of the produced biodiesel are listed in Table 2.

2.3. Test equipment

The equipment used in this study are listed in Table 3.

2.3.1. Working principle of high frequency reciprocating friction and wear tester

The working principle of the high frequency reciprocating friction and wear tester is shown in Fig. 1. The test oil sample (2 mL) is placed in an oil bath at a given temperature. The steel ball fixed in the fixture vertically loads the horizontally installed steel sheet. The ball reciprocates at a frequency of 50 Hz and a stroke of 1000 μm, the test load is 200 g, the test temperature is 60 °C, and the contact interface between the test ball and the test piece is completely immersed in the oil. According to the test environment

Table 2 – Physicochemical properties of the biodiesel used in this study.

Number	Sample	Kinematic viscosity at 40° (mm^2/s)	Cetane number (min)	Flash point (°)	Density (kg/m^3)	Water content (%)	Carbon residue (%)	Sulfur content (%)
1	SSME	4.22	46.7	162	868.2	0.092	0.048	0
2	JME	4.06	51	164	862.0	0.081	0.046	0.041
3	COSME	4.54	52.3	150	874.5	0.086	0.38	0.046
4	MME	4.30	47.4	170	867.4	0.083	0.038	0.033
5	OSME	3.24	55.7	152	876.4	0.084	0.047	0.034
6	CME	4.53	54.3	178	875.2	0.088	0.003	0.039
7	RME	4.63	48.00	163	884.8	0.096	0.023	0.046
8	SME	4.20	50.48	170	867.2	0.086	0.023	0.042
9	PME	5.06	58.41	174	877.1	0.087	0.036	0.043
10	PAME	4.35	52.34	165	882.2	0.035	0.032	0.052
11	SBME	4.12	51.80	159	884.6	0.091	0.02	0.027
12	RSME	4.79	50.40	158	862.3	0.069	0.046	0.042
13	OME	5.05	58.70	171	876.2	0.079	0.029	0.045
14	OOB	5.83	51.48	176	880.6	0.031	0.051	0.065

Table 3 – Test equipment.

Test equipment	Manufacturer	Country
Gas chromatograph	Agilent Technologies 7890A	United States
High frequency reciprocating friction and wear testing machine	Meryer	Shanghai, China
Purelab Classic	Elga Lab Water	Britain
XS205DU electronic balance	Mettler Toledo	Switzerland
R-215 rotary evaporator	Buchi	Switzerland
SK5200HP Ultrasonic Cleaner	Kudos	Shanghai, China
Constant temperature drying oven.	Chongming Experimental Instrument Factory	Shanghai, China

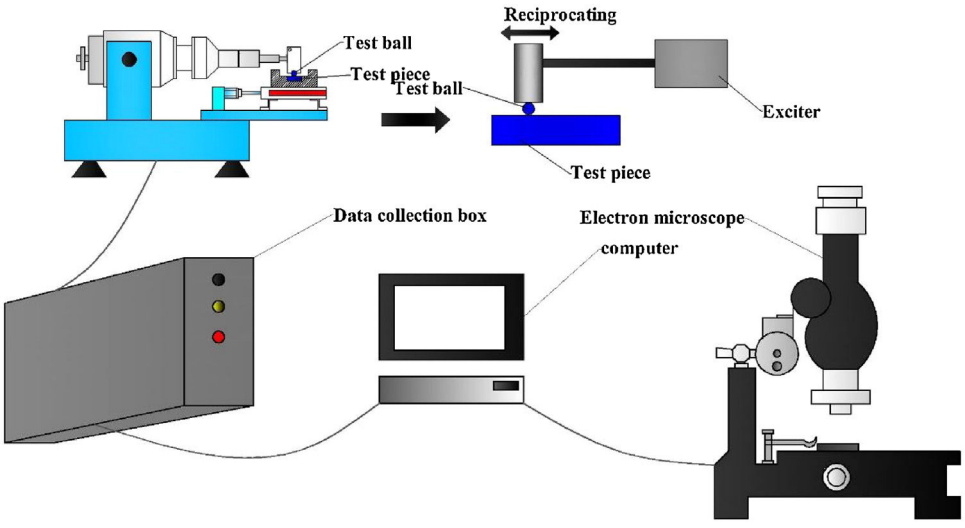

Fig. 1 – Schematic illustration of high frequency reciprocating friction and wear tester.

(temperature and humidity), the wear scar diameter of the steel ball was corrected to the value under the standard condition. The lubricity of the test sample was expressed by the corrected wear scar diameter. The wear scar diameter mentioned in this study was corrected wear spot diameter.

2.3.2. *Calculation of test data*

The measured wear spot diameter needs to be corrected according to the water vapor pressure of 1.4 kPa. The corrected wear spot diameter is expressed by using WS1.4. The calculation method is as follows [22]:

(1) Unadjusted average wear spot diameter is expressed in MWSD (μm) and is calculated as follows:

$$\mathrm{MWSD} = \frac{X + Y}{2}$$

where X is the vertical wear scar diameter in the direction of vibration (μm); and Y is the horizontal wear scar diameter in the direction of vibration (μm).

Table 4 – The abrasive spot diameters of fourteen types of biodiesel and diesel.

Number	Sample	Abrasive spot diameter (μm)
1	SSME	180.99
2	JME	177.44
3	COSME	176.89
4	OSME	185.16
5	MME	181.27
6	CME	184.62
7	RME	186.47
8	SME	182.14
9	PME	169.97
10	SBME	179.15
11	RSME	169.71
12	OME	171.84
13	OOB	175.58
14	PAME	187.35
15	0# diesel	365.35

(2) Absolute vapor pressures (AVP_1 and AVP_2) at the beginning and end of the test. The mean absolute vapor pressure (AVP) during the experiment is calculated as follows:

$$AVP_1 = \frac{RH_1 - 10v1}{750}$$

$$AVP_2 = \frac{RH_2 - 10v2}{750}$$

$$AVP = \frac{AVP_1 + AVP_2}{2}$$

where RH_1 is the relative humidity of the incubator at the beginning of the test and RH_2 is the relative humidity of the incubator at the end of the test expressed in percentage. The calculation formulas for v1 and v2 are as follows:

$$v1 = 8.017352 - \frac{1705.984}{231.864 + t1}$$

$$v2 = 8.017352 - \frac{1705.984}{231.864 + t2}$$

where t1 is the temperature of the incubator at the beginning of the test and t2 is the temperature of the incubator at the end of the test.

(3) WS1.4 is calculated as follows:

$$WS1.4 = MWSD + HCF\,(1.4 - AVP)$$

Note: For unknown oil samples, the HCF value is 60.

3. Results and discussion

3.1. *Lubrication performance of biodiesel*

A high-frequency reciprocating friction and wear tester was used to measure the abrasive spot diameters of biodiesel and 0# diesel according to the ISO 12156-1 standard. The results are presented in Table 4.

Table 4 summarizes that RSME has the smallest abrasive spot diameter of 169.71 μm. Compared to 0# diesel, biodiesel has a lower abrasive spot diameter, which is attributed to the fact that the composition of biodiesel is mainly composed of FAMEs. Table 5 presents that the main components of 14 types of biodiesel are methyl stearate, methyl palmitate, methyl oleate, methyl linoleate, and the average content of four components reached 92.18%, of which the content of methyl oleate and methyl linoleate was the largest, with the average of 79.37%, and others were relatively small. The selection of biodiesel is aimed at representing the entire saturated–unsaturated and monounsaturated–polyunsaturated FAME ranges as illustrated in the ternary plot in Fig. 2. Biodiesel contains a polar functional ester group, and polar molecules are more easily adsorbed on the metal surface to form a physical adsorption membrane [23]. At the same time, residual glycerol monoester and diglyceride during biodiesel production affect the lubricating properties of biodiesel. Importantly, some studies have shown that changes in the concentration of monoglycerides have a significant positive effect on the biodiesel lubricity [24,25]; therefore, lubricity of biodiesel is better than that of 0# diesel.

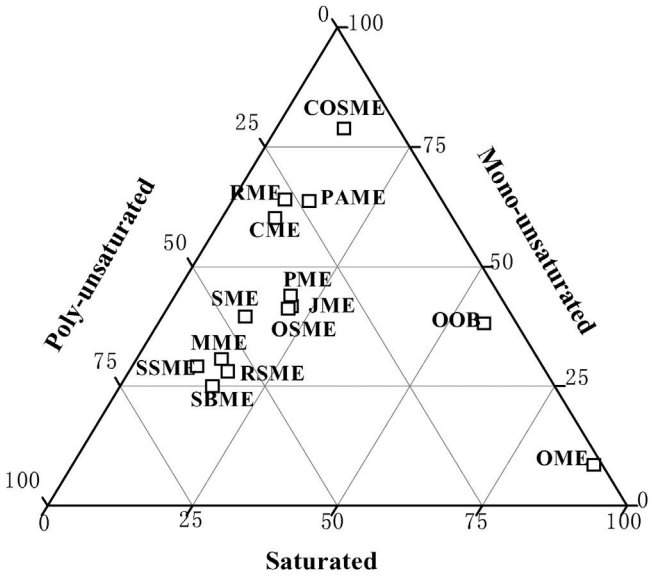

Fig. 2 – Ternary plot describing the FAME composition of the tested biodiesels.

3.2. *The abrasive spot diameter of the four main components of biodiesel*

Fig. 3 presents the values of abrasive spot diameter of RSME, methyl palmitate ($C_{16:0}$), methyl oleate ($C_{18:1}$), methyl linoleate ($C_{18:2}$), and methyl stearate ($C_{18:0}$). Fig. 3 exhibits that the abrasive spot diameters of $C_{18:1}$ and $C_{18:2}$ containing carbon–carbon double bonds are significantly smaller than that of $C_{18:0}$, which indicates that the carbon–carbon double bond has positive impact on the lubricating performance of biodiesel. The main factor influencing the lubricating performance is the strength of the adsorption membrane. The stronger the intermolecular binding in the adsorption membrane, the stronger the stability and the compactness of the adsorption membrane. The intermolecular interaction in the adsorption membrane is mainly electrostatic. The greater the number of double bonds, the greater the electrostatic force [26]. The double bonds make it easier for fatty acid esters

Table 5 – Main composition of 14 types of biodiesel.

FAME	$C_{16:0}$	$C_{16:1}$	$C_{18:0}$	$C_{18:1}$	$C_{18:2}$	$C_{18:3}$	$C_{20:1}$	$C_{20:0}$	$C_{22:0}$	$C_{22:1}$	C_{others}
SSME	6.76	0.00	3.48	28.13	59.36	0.25	0.29	0.00	0.02	0.71	1.00
JME	14.29	0.00	7.02	41.70	36.99	0.00	0.00	0.00	0.00	0.00	0.00
COSME	8.58	0.00	2.22	78.80	9.44	0.00	0.00	0.68	0.00	0.00	0.28
OSME	16.91	0.24	1.55	40.27	36.94	0.90	0.66	0.83	0.00	0.00	1.70
MME	12.61	0.00	1.74	30.16	53.97	0.67	0.44	0.41	0.00	0.00	0.00
CME	4.27	0.24	2.49	57.33	23.55	6.57	0.69	1.58	0.62	0.90	1.74
RME	1.60	0.27	1.85	59.38	19.82	6.35	0.76	1.65	0.80	1.63	2.89
SME	8.74	0.00	5.65	38.87	45.67	0.41	0.65	0.00	0.00	0.00	0.00
PME	11.46	0.00	4.08	42.14	36.05	0.00	1.80	1.04	3.42	0.00	0.00
SBME	11.08	0.00	3.90	24.21	53.14	5.35	0.50	0.00	0.94	0.00	0.69
RSME	9.50	0.44	7.58	27.22	35.82	19.04	0.41	0.00	0.00	0.00	0.00
OME	10.82	3.05	79.30	5.00	0.57	0.86	0.41	0.00	0.00	0.00	0.00
OOB	18.93	7.35	31.37	30.00	4.13	1.50	0.67	1.08	1.09	0.08	3.79
PAME	4.13	0.31	1.90	48.61	16.22	6.61	0.97	4.39	0.99	13.37	2.48

Note: $C_{m:n}$ denotes FAME; where m indicates the number of carbons of the fatty acid; n represents the number of C=C bonds, and C_{other} indicates the rest untested components.

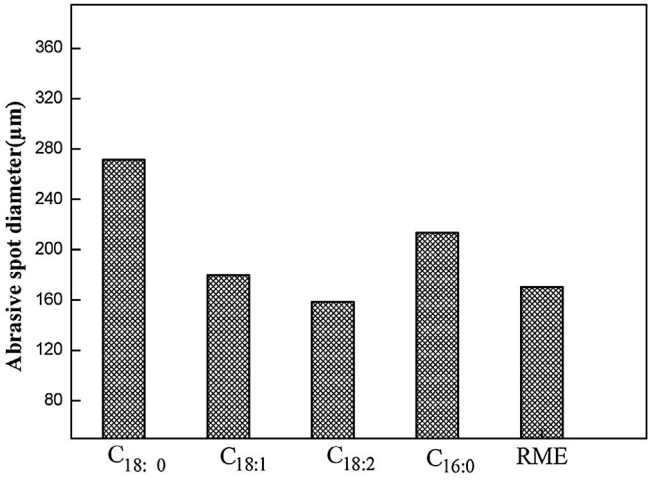

Fig. 3 – Abrasive spot diameter of biodiesel and its four main components.

to form a dense adsorption film on the metal surface, which increases the strength of the lubricating film. This is also consistent with previous research results [27].

The above mentioned results only explain the reasons for the change in the lubricating properties of the main components of biodiesel. Fig. 2 demonstrates that there is no significant relationship between the number of double bonds in the structure of biodiesel and the lubricating performance. Therefore, analysis of the quality of biodiesel lubrication presented in Table 2 will be pursued in further study.

3.3. *Quantitative relationship between the biodiesel composition and its corrected abrasive spot diameter*

$C_{18:0}$, $C_{18:1}$, $C_{18:3}$, $C_{16:1}$, $C_{20:1}$, $C_{20:0}$, $C_{22:0}$, $C_{16:0}$, $C_{22:1}$, and C_{other} were used as independent variables, and the biodiesel calibration spot diameter was used as the dependent variable. The multiple linear regression analysis method was used to build up the corrected abrasive spot diameter prediction model based on the biodiesel composition as follows:

Table 6 – Statistical analysis of the model regression equation.

Sample size	Correlation coefficient R	F test	Significance test
60	0.91	29.32	$\ll 0.01$

$$d = 184.58 - 0.55C_{18:0} - 0.05C_{18:1} - 0.13C_{18:3} - 5.4C_{16:1} - 1.1C_{20:1} + 0.63C_{20:0} - 1.53C_{22:0} - 0.12C_{16:0} + 0.11C_{22:1} + 2.6C_{other}$$

where $C_{18:0}$, $C_{18:1}$, $C_{18:3}$, $C_{16:1}$, $C_{20:1}$, $C_{20:0}$, $C_{22:0}$, $C_{16:0}$, $C_{22:1}$, and C_{other} correspond to stearic methyl ester, oleic methyl ester, linolenic methyl ester, palmitic methyl ester, palmitoleic methyl ester, eicosenoic methyl ester, arachidic methyl ester, behenic methyl ester, palmitic methyl ester, and erucic methyl ester, respectively; and C_{other} represents the sum of the contents of wood acesuic acid methyl ester and other unknown components. D is the corrected abrasive spot diameter of biodiesel. The main statistical analysis results of the regression analysis equation are listed in Table 6.

Table 6 summarizes that the correlation coefficient (R = 0.91) was significantly higher than the statistically significant zero-order value (R_{min} = 0.281). Therefore, the corrected spot diameter (d) of biodiesel has a significant correlation with the ten established variables, thereby indicating that the model is feasible. The results of the model are as follows: F = 29.32, significance $\ll$0.01, thereby revealing a significant effect of the model in describing the linear relationship between the corrected abrasive spot diameter of biodiesel and the independent variables. The ten-step linear regression analysis method was thus found to be reliable. The linear regression coefficient indicates that the first order of the influencing factors of the correction abrasive spot diameter of biodiesel was $C_{16:1} > C_{22:0} > C_{20:1} > C_{18:0} > C_{18:3} > C_{16:0} > C_{18:1}$. The correlation coefficients of $C_{16:0}$ and $C_{18:3}$ were low; therefore, the corrected abrasive spot diameter of biodiesel was not reduced and $C_{other} > C_{20:0} > C_{22:1}$. The FAME percentage composition of the biodiesel predicted its corrected

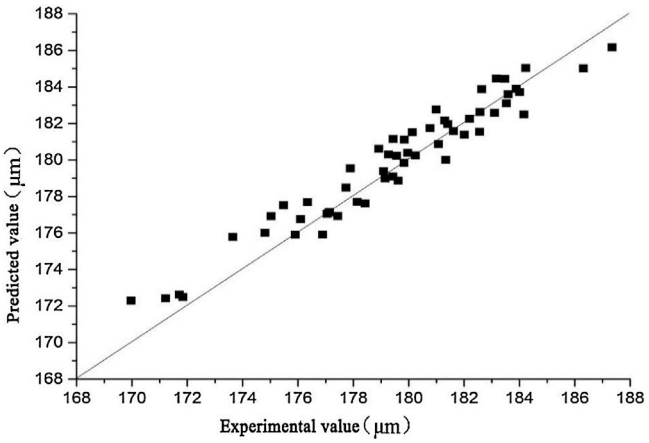

Fig. 4 – Calculated versus measured values based on the regression model.

abrasive spot diameter. The deviation between the predicted and the experimental values is shown in Fig. 4.

Fig. 4 exhibits that 60 data points are evenly distributed on both sides of the diagonal, and most of the experimental–predicted value gaps are less than 1.5 μm (within the test error range). The significance level of the correlation coefficient is 0.01, and it is clear that the experimental values are highly correlated with the predicted values. The regression model can predict the corrected abrasive spot diameter of biodiesel based on its FAME composition.

4. Conclusions and future prospects

(1) The main components of the 14 types of biodiesel are methyl stearate, methyl oleate, methyl linoleate, and methyl palmitate. The average content of the four components is 92.18%. Among 14 biodiesel oil samples, rubber seed oil biodiesel exhibits the smallest wear scar diameter, which is 169.71 μm. Zanthoxylum oil has the largest wear scar diameter of 187.35 μm.

(2) The carbon–carbon double bonds make it easier for fatty acid esters to form a dense adsorption film on the metal surface, which increases the strength of the adsorption film and improves the lubricating properties of biodiesel.

(3) A highly linear correlation prediction model for the biodiesel induction period was established. Based on the chemical composition of the feedstock oil or the biodiesel sample, the corrected abrasive spot diameter of biodiesel can be directly predicted. This method is highly convenient for the application and research of biodiesel. Moreover, this methodology provides the basis for the promotion and application of biodiesel in different environments.

5. Future prospects

The composition of biodiesel is very complex and exploration of the lubrication mechanism of biodiesel is difficult. In future study, scanning electron microscopy or optical microscopy will be employed to obtain the images of the wear tracks in order to explain the related mechanism in detail.

Conflicts of interest

The authors declare no conflicts of interest.

Acknowledgements

The authors greatly acknowledge the support provided by the National Natural Science Foundation of China (51766007), NSFC-Yunnan Joint Fund Project (U1602272), and Research Fund from State Key Laboratory of Complex Nonferrous Metal Resources Clean Utilization (CNMRCUTS1704).

REFERENCES

[1] Ahmed S, Hassan MH, Kalam MA, Ashrafur Rahman SM, Abedin MJ, Shahir A. An experimental investigation of biodiesel production, characterization, engine performance, emission and noise of *Brassica juncea* methyl ester and its blends. J Clean Prod 2014;79(18):74–81.

[2] Senthil R, Sivakumar E, Silambarasan R. Effect of di ethyl ether on the performance and emission characteristics of a diesel engine using biodiesel–eucalyptus oil blends. RSC Adv 2015;5(67):54019–27.

[3] Watts N. The 2018 report of the Lancet Countdown on health and climate change: shaping the health of nations for centuries to come. Lancet 2018;392(10163):2479–514.

[4] Watts N. Countdown on health and climate change: from 25 years of inaction to a global transformation for public health. Lancet 2018;391(10120):581–630.

[5] Montgomery H. Preventing the progression of climate change: one drug or polypill? Biofuel Res J 2017;4(1):536.

[6] Aghbashlo M, Tabatabaei M, Hosseinpour S. On the exergoeconomic and exergoenvironmental evaluation and optimization of biodiesel synthesis from waste cooking oil (WCO) using a low power, high frequency ultrasonic reactor. Energy Convers Manage 2018;164:385–98.

[7] Mahmudul HM, Hagos FY, Mamat R, Adam AA, Ishak WFW, Alenezi R. Production, characterization and performance of biodiesel as an alternative fuel in diesel engines — a review. Renew Sustain Energy Rev 2017;72:497–509.

[8] Aghbashlo M, Tabatabaei M, Rastegari H, Ghaziaskar HS. Exergy-based sustainability analysis of acetins synthesis through continuous esterification of glycerol in acetic acid using Amberlyst®; 36 as catalyst. J Clean Prod 2018.

[9] Kumar Niraj. Oxidative stability of biodiesel: causes, effects and prevention. Fuel 2016.

[10] Fazal MA, Haseeb ASMA, Masjuki HH. Investigation of friction and wear characteristics of palm biodiesel. Energy Convers Manage 2013;67(67):251–6.

[11] Kumar Niraj, Varun, Chauhan S. Analysis of tribological performance of biodiesel. Proc Inst Mech Eng J 2014;228:797–807.

[12] Luo H, Fan W, Li Y, Nan G. Biodiesel production using alkaline ionic liquid and adopted as lubricity additive for low-sulfur diesel fuel. Bioresour Technol 2013;140(3):337–41.

[13] Aline Cristina Mendes De Farias, Alves SM. Micro and nanometric wear evaluation of metal discs used on determination of biodiesel fuel lubricity. Mater Res 2014;17(8):89–99.

[14] Lapuerta, Magín, Sánchez-Valdepe?as, Jesús, Bolonio D, Sukjit E. Effect of fatty acid composition of methyl and ethyl esters on the lubricity at different humidities. Fuel 2016;184:202–10.
[15] Sulek MW, Kulczycki A, Malysa A. Assessment of lubricity of compositions of fuel oil with biocomponents derived from rape-seed. Wear 2010;268(1):104–8.
[16] Xiao H, Zou H, Liu S, Li C. An investigation of the friction and wear behavior of soybean biodiesel. Tribol Int 2019;131:377–85.
[17] Sukjit E, Tongroon M, Chollacoop N, Yoshimura Y, Poapongsakorn P, Lapuerta M, et al. Improvement of the tribological behaviour of palm biodiesel via partial hydrogenation of unsaturated fatty acid methyl esters. Wear 2019;426:813–8.
[18] Chourasia S, Patel PD, Lakdawala A, Patel RN. Study on tribological behavior of biodiesel–diethyl ether (B20A4) blend for long run test on compression ignition engine. Fuel 2018;230:64–77.
[19] Knothe Gerhard. Improving biodiesel fuel properties by modifying fatty ester composition. Energy Environ Sci 2009;2.
[20] Hosseinpour Soleiman, Hosseinpour S, Aghbashlo M, Tabatabaei M, Khalife E. Exact estimation of biodiesel cetane number (CN) from its fatty acid methyl esters (FAMEs) profile using partial least square (PLS) adapted by artificial neural network (ANN). Energy Convers Manage 2016;124:389–98.
[21] Geller Daniel P, Goodrum JW. Effects of specific fatty acid methyl esters on diesel fuel lubricity. Fuel 2004;83(17):2351–6.
[22] Yan Shude, Zhu Min. Determination of diesel lubricity by high frequency reciprocating tester. Contemp Chem 2006;35(1):50–2.
[23] Hu J, Du Z, Li C, Min E. Study on the lubrication properties of biodiesel as fuel lubricity enhancers. Fuel 2005;84:1601–6.
[24] Knothe Gerhard, Steidley KR. Lubricity of components of biodiesel and petrodiesel. The origin of biodiesel lubricity†. Energy Fuels 2005;19(3):1192–200.
[25] Wain KS, Perez JM, Chapman E, Boehman AL. Alternative and low sulfur fuel options: boundary lubrication performance and potential problems. Tribol Int 2005;38:313–9.
[26] Niu Xiaomin. Investigation of the performance of low sulfur diesel lubricant additives and the research of new additives. Diss. East China University of Science and Technology; 2012.
[27] Fox NJ, Tyrer B, Stachowiak GW. Boundary lubrication performance of free fatty acids in sunflower oil. Tribol Lett 2004;16(4):275–81.